HHS Public Access

Author manuscript

Chemosphere. Author manuscript; available in PMC 2024 August 01.

Published in final edited form as:

Chemosphere. 2023 August ; 332: 138811. doi:10.1016/j.chemosphere.2023.138811.

Comparative Evaluation of Filtration and Imaging Properties of Analytical Filters for Microplastic Capture and Analysis

Jared Carter[1], **Teagan Horan**[1], **Joshua Miller**[1], **Gregory Madejski**[2], **Erin Butler**[1], **Corinne Amato**[1], **James Roussie**[1,*]

[1]SiMPore Inc., 150 Lucius Gordon Drive, Suite 110, West Henrietta, NY 14586

[2]University of Rochester, Rochester, NY

Abstract

Pollution by microplastics (MPs) is a growing problem that is now well-recognized, as concerning levels of MPs have been found in drinking water, food, and even human tissues. Given the evolving understanding of their toxicological effects on human health, MPs are an area of concern requiring further study. Consequently, there is a need for greater understanding of the performance characteristics of common MP analytical methods and where possible, for standardizing methods and reporting practices. Here, we report our work comparing filtration and imaging properties of five analytical filters suitable for MP capture and analysis. We compared track-etched polycarbonate with (PCTEG) and without gold coating (PCTE), polytetrafluoroethylene (PTFE), porous silicon (PSi), and gold-coated microslit silicon nitride membranes (MSSN-Au). Four of the filter types had a nominal 1.0 μm cut-off, except for PCTEG which had a 0.8 nominal cut-off. We examined the ultrastructure of each membrane type by electron microscopy to understand how their physical properties influence filtration and imaging performance. We compared clean water filtration rates and timed volume passage for each filter in comparison to its porosity and working surface area. We further compared optical microscopy imaging properties for each filter with model MP samples in both bright-field and fluorescent modes with accompanying Nile Red staining. In terms of absolute and surface area-normalized flow rates, our measurements ranked the filters in order of MSSN-Au > PTFE > PCTE > PCTEG > PSi. Similarly, we found MSSN-Au filters compared favorably in terms of optical microscopy performance. Collectively, these data will aid practitioners when choosing analytical filters for MP surveillance and testing.

Graphical Abstract

*Corresponding Author; Address: SiMPore Inc., 150 Lucius Gordon Drive, Suite 110, West Henrietta, NY 14586; jroussie@simpore.com; Phone: +1 (585) 214-0585.

Author Contributions

JC, JR: Conceptualization; Supervision; Funding acquisition; Original draft; Review & editing. JM, GM, EB, CA: Investigation; Methodology. TH: Data curation; Formal analysis; Investigation; Methodology; Original draft; Review & editing.

Declaration of interests

JR is a co-founder and equity holder of SiMPore Inc.

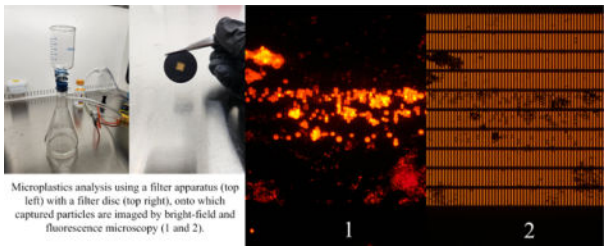

Microplastics analysis using a filter apparatus (top left) with a filter disc (top right), onto which captured particles are imaged by bright-field and fluorescence microscopy (1 and 2).

Keywords

Microplastics; Analytical Methods; Filtration; Optical Microscopy

1. Introduction

Pollution by microplastics (MPs) is a growing problem now being recognized by the scientific community and regulatory bodies as a contaminant of emerging concern. Concerning levels of MPs have been found in drinking, fresh and ocean waters (1), food and beverages (2), and even human tissues (3–5). Given the evolving understanding of their immediate and long-term toxicological effects on human health (6, 7), MPs are an area of concern requiring further study. Consequently, there is a need for greater understanding of the performance characteristics of common MP analytical methods and where possible, for standardizing methods and reporting practices (1, 8, 9).

A number of methodologies have evolved over the past decade for the analysis of MPs, including optical microscopy, Raman and infrared spectroscopy, and pyrolysis-gas chromatography-mass spectrometry among the leading and most often cited methods (10). As previously noted, there is a lack of standardization regarding data collection and reporting. Thus, there remains a need to harmonize all aspects of MP analysis work streams, which in many cases, requires a more detailed understanding of the fundamental performance characteristics of related tools and factors affecting analytical outcomes.

One common theme among analytical methodologies is the capture and on-filter analysis of MPs, particularly for procedures that rely on optical microscopy and Raman or infrared spectroscopy. Here, we report our work comparing the filtration and imaging properties of five analytical filters suitable for MP capture and analysis. This comparison was undertaken as part of an interlaboratory methods evaluation study coordinated by the Southern California Coastal Water Research Project (9). All of these filters have been previously used to characterize field samples for MP content, and often, are used as the analytical filter onto which particles are vacuum filtered for optical microscopy end-point measurements following recovery of particles collected on stainless steel mesh filters from large volume field samples. We compared track-etched polycarbonate with (PCTEG) and without gold coating (PCTE), polytetrafluoroethylene (PTFE), porous silicon (PSi), and gold-coated microslit silicon nitride membranes (MSSN-Au). We examined the ultrastructure of each membrane type by electron microscopy to understand how their physical properties influence filtration and imaging performance. We compared clean water filtration rates and timed volume passage for each filter in comparison to its porosity and

working surface area. We further compared optical microscopy imaging properties for each filter with model MP samples in both bright-field and fluorescent modes with accompanying Nile Red staining. We rank our results in terms of best water permeance and optical microscopy characteristics and discuss how practitioners may weight these factors when choosing analytical filters for MP analysis. Collectively, our data presented here will aid practitioners when choosing filter membranes for MP surveillance and testing.

2. Materials and Methods

2.1. Filter Membranes:

A total of five different filter types were examined as part of this study. Four filters were commercially sourced from vendors and a fifth type was internally developed and fabricated (see below). Commercially supplied filters were used as received without any modification nor any pre-treatment. These filters included polytetrafluoroethylene (PTFE), porous silicon (PSi), and two track-etched polycarbonate types: 1) with 40 nm thick gold coating (PCTEG), and 2) without gold (PCTE). PCTEG, PCTE, and PTFE were purchased from Sterlitech Inc, while PSi was purchased from Smart Membranes GmbH. Except for PCTEG, which had a nominal 0.8 μm cut-off, all filters had a nominal 1.0 μm cut-off. PTFE, PCTEG, and PCTE membranes were supplied as 25 mm diameter discs, while PSi and MSSN-Au required an additional 25 mm silicone layer (with a cut central opening) as supports. Table 1 summarizes key properties for all five filters.

2.2. MSSN-Au Filter Fabrication:

The MSSN-Au membranes were fabricated per our previously reported methods (11). Briefly, 1 × 50 μm slit pores were initially patterned on the frontside of a silicon wafer, within a 400 nm-thick silicon nitride layer on 150 mm diameter, 310 μm thick, double-side polished silicon wafers (WaferPro Inc.). Conventional photolithography patterning and reactive ion etching were used to transfer the slit pores into the silicon nitride. After fabrication of frontside pores, the wafers' backside was processed for bulk through-wafer etching. Resultant freestanding membranes were then coated with a targeted 2 nm thick Cr adhesion layer and a 120 nm thick gold layer by an e-beam evaporator system (CHA Industries Inc.). Each processed wafer yielded approximately 400 MSN-Au membrane chips with three 0.7 × 3 mm porous suspended membranes (~520 nm thick) and were used without any further modifications. An 8 μm cut-off MSSN variant lacking gold coating was used previously for studying the entrainment of MPs along a municipal drinking water system (12).

2.3. Scanning Electron Microscopy:

An Auriga field emission SEM (Carl Zeiss Vision Inc.), outfitted with a custom holder for sample manipulation by a Kleindiek 3-axis probe, was used for routine quality inspections of internally fabricated MSSN-Au membranes and for collection of top-down and cross-sectional imaging of all five membrane types. Cross-sections were created by either simple fracture (PSi, MSSN-Au) or by razor blade cleavage (PTFE, PCTE, PCTEG). PTFE, PCTE, and PSi membranes were deposited with ~7 nm Au coating to enhance surface contrast and reduce charging during SEM, using a DESK-II DC sputtering system (Denton Vacuum

LLC). Resultant micrographs are presented in Figure 1 as collected. For MSSN-Au, NIH Image J was used to calculate pore properties (settings of threshold - 62; pixel size - 100 - infinity).

2.4. Cleaning and Contamination Mitigation:

Personnel wore white 100% cotton lab coats and nitrile gloves when cleaning and handling all materials and when filtering samples. All filtration processes were conducted in a laminar flow hood and surfaces of hoods were cleaned with 70% isopropanol and wiped dry with natural fiber Kimwipes. Vacuum filtration funnels, storage bottles, and stainless-steel tweezers were rinsed 3-times with tap water, then 3-times with particle-free water, and dried in the laminar flow hood (Laminar Flow Cabinet, Air Science LF Series). Between uses with different filters, all glassware, gaskets, and tweezers were similarly rinsed and dried.

2.5. Water Permeance Measurements:

For all water flow rate measurements and preparation of bead suspensions (see below), particle-free water was used and produced from reverse-osmosis feed water post–conditioned by a Barnstead Inc. Nanopure water system to a minimum resistivity of 18.2 mΩ/cm, then filtered sequentially through two 0.2 μm cut-off PES bottle-top filters (Thermo Fisher Corp.). Vacuum filtration was performed using an all-glass vacuum filtration apparatus (Fisherbrand 09–753E) and house-generated internal vacuum (~97.9 kPa gauge pressure). When loaded on the filtration apparatus' glass frit, the PCTEG, PCTE, PTFE, and MSSN-Au filters were sandwiched between two 500 μm-thick in-house cut silicone O-ring-like gaskets to maintain a fluidic seal. The gaskets had a 12.5 mm diameter central opening to permit water flow and effective surface area values reported in Table 2 are based on this dimension for PTFE, PCTE, and PCTEG membranes. All gaskets were handled with cleaned stainless-steel tweezers (ideal-tek, SM111.SA.1). Gaskets used with PSi membranes were supplied by the vendor. One-liter volumes of particle-free water were analyzed in triplicate for each filter type and the processing time recorded for passage of each one-liter sample.

2.6. Bead Suspensions and Filtration:

3–10 μm diameter PMMA beads (0.95 μg/mL stock suspension; Cospherics Inc.) were diluted 1:100 into particle-free water. One-mL volumes were pipetted directly onto various filters assembled in the vacuum apparatus and the vacuum applied until the entire volume passed and the filter was dried. The diluted bead suspension was thoroughly mixed before each use to ensure its homogeneity.

2.7. Nile Red Staining:

Once the filtration was run to dryness, the vacuum was turned off and then 1 mL of 1 μg/mL (w/v in particle-free water) Nile Red solution was directly pipetted onto the filter. After a 10-minute incubation, the solution was filtered off by re-applying the vacuum and then the filter was rinsed in 1 mL of 0.2 μm-filtered 99% isopropanol, dried under vacuum, and finally transferred to darkened boxes for subsequent storage and microscopy. The 1 μg/mL

Nile Red solution was prepared for each use by diluting from a stock of 1 mg/mL Nile Red solution (w/v in 0.2 μm-filtered 99% ethanol).

2.8. Optical Microscopy:

Images were captured using an inverted Nikon Eclipse TS100 microscope equipped with an AmScope digital camera (MU1203-FL), with image processing conducted using the associated AmScope 3.7 software. Images were captured in three distinct modes: 1) bright-field with white light illumination, 2) fluorescent illuminated green excitation, and 3) fluorescent green excitation. Green channel fluorescence was collected using a conventional fluorescein excitation and emission filter set. Illuminated green excitation was used to identify where on a given filter a particle was located, while green excitation without background illumination was used to identify Nile Red-stained particles. Exposure time and camera gain varied by filter type and these data are reported along with representative images in Figure 2.

2.9. Chemicals and Solvents:

Throughout this study, unless otherwise specified, routine solvents and chemicals were purchased from either Sigma-Aldrich or Thermo Fisher at analytical grade or higher purity.

3. Results

3.1. Filter Properties Revealed by SEM Analysis:

As shown in Figure 1, top-down and cross-sectional SEM imaging revealed differences in the ultrastructure of the filters we examined. All polymeric membranes appeared to be approximately 30 μm or less in thickness. PCTE, PCTEG, and PTFE membranes demonstrated well-recognized tortuous-path pore geometries. While the pores of PTFE had a stretched fibrous-looking structure, the pores of PCTE and PCTEG showed singlet and multiplet structures. As compared to its gold-coated counterpart, the PCTE membranes showed a high degree of charging during imaging (despite being coated with ~7 nm thick Au), displaying bright spots on the surface and within the side walls of angled pores. These distortions made characterizing the native PCTE membrane challenging. The gold coating (as supplied by the vendor) on PCTEG showed a marked decrease in pore size (0.8 μm vs. 1.0 μm comparing PCTEG and PCTE), with a commensurate decrease in porosity (15% and 16% for PCTEG and PCTE, respectively). There were fewer bright spots on PCTEG micrographs that seemed mostly confined within the side walls of pores, suggesting that its 40 nm thick gold layer helped dissipate charging under the electron beam during imaging.

In contrast, the two inorganic membranes (PSi and MSSN-Au) both had straight-through pore geometries, with rounded-square pores for PSi and long rectangular prism pores for MSSN-Au. The gold coating on MSSN-Au membranes appeared as a conformal layer on all pore surfaces. Further, MSSN-Au membranes appeared to be ~440-times thinner than PSi membranes (0.5 μm vs. 220 μm, respectively). Analysis of MSSN-Au micrographs were used to populate its associated filter properties in Table 1.

3.2. Water Permeance Measurements:

Table 2 summarizes our observations for timed passage of one-liter water samples and further reports flux rates in absolute and membrane surface area-normalized terms. Polymeric membranes (PTFE and PCTE) demonstrated similar passage times, absolute flux rates, and surface area-normalized flux rates, as these two filters had relatively similar membrane properties. However, the addition of gold to PCTE (i.e., PCTEG) markedly changed these observed measures, as the one-liter passage time increased by ~4.0-fold with a commensurate ~4.0-fold decrease in absolute and surface area-normalized flux rates, when comparing PCTEG to PCTE. The longest one-liter passage time and the slowest flux rates were observed for PSi membranes; i.e., PSi flux rates were ~19.0-fold lower than the polymeric membrane with the fastest flux rates (PTFE) and ~23.2-fold lower than those for the other inorganic membrane (MSSN-Au). Finally, making similar comparisons between PTFE and MSSN-Au revealed interesting results. Despite MSSN-Au having ~19.5-fold less effective membrane surface area than PTFE, MSSN-Au demonstrated ~1.2-fold higher absolute and ~23.7-fold higher surface area-normalized flux rates versus PTFE. Comparing across all five filter types, our measurements ranked the filters in order of MSSN-Au > PTFE > PCTE > PCTEG > PSi for water permeance measurements. We also attempted to compare our results to vendor-supplied water flow rates, but either they were unavailable or were collected at a different applied pressure, which makes such comparisons impossible or uninformative.

3.3. Optical Microscopy Performance:

Figure 2 shows representative bright-field and fluorescent micrographs for all five filter types with Nile Red-stained, 3–10 μm diameter PMMA beads. The exposure time and camera gain settings for acquisition of the fluorescent micrographs are also shown in Figure 2 since they varied considerably between filter types. These data show that there were pronounced variations in the optical behavior of the membranes we examined. Our observations found PTFE background auto-fluorescence prevented use of higher gain to improve contrast, limiting the image resolution of captured particles. Moreover, PTFE membranes appeared bright red, with occasional brighter streaks, presumably due to retention of the Nile Red stain. Unavoidable wrinkling induced during filtration caused changes in planarity as well. In a given field of view, sections of the membrane remained out of focus in all imaging modes. Wrinkling also occurred to a lesser degree with PCTE and PCTEG membranes.

Bright-field micrographs of PCTE and PCTEG membranes appeared similar in structure, with a high-contrast, speckled pattern. Under bright-field observation, this pattern easily camouflaged the presence of any retained 3–10 μm PMMA beads, with only larger and irregularly shaped particles easily identified. These large, irregular particles appeared to be at least 20 μm in at least one dimension and are likely extraneous contaminants. All three polymeric membranes (PTFE, PCTE, and PCTEG) demonstrated similar behavior, with retained PMMA particles invisible under bright-field and apparent under fluorescence. The autofluorescence of the PCTE membrane limited confident particle differentiation, as strongly fluorescent particles were surrounded by a halo of scattered light. The gold coating on PCTEG membranes clearly improved fluorescent imaging performance, without any

similar light halo observed under fluorescence. Both PSi and MSSN-Au membranes showed little to no auto-fluorescence and particles were readily distinguished in all imaging modes. The scale of captured particles was apparent against the regularly shaped slit features of the MSSN-Au membranes, while the background of PSi membranes were highly consistent and free of distinguishing features under the imaging conditions we examined.

4. Discussion

This study undertook a comparison of the filtration and optical imaging properties of five analytical filters for use in MP capture and analysis applications. These five filters included PTFE, PCTE, PCTEG and PSi membranes commonly used for this purpose (8, 10) and included novel MSSN-Au membranes, where a non-gold-coated MSSN variant had been previously used for non-spectroscopic MP analysis (12). Except for PCTEG, which had a nominal 0.8 μm cut-off, all filters had a nominal 1.0 μm cut-off. Relevant to methodological harmonization, similar 1.0 μm cut-off filters are recommended in standardized protocols for MP analysis in the California State Water Resource Control Board's policy handbook (released 8/9/2022).

Similar to other protocols (13), the California protocol describes collection of large volume field samples on large surface area filters (e.g. stainless steel mesh with specified cut-off), then recovery and transfer of collected particles via vacuum filtration onto analytical filters like those studied here. The protocol further specifies optical microscopy measurements (i.e., particle number, morphology, size, and color). Both the clean water and particle challenge/microscopy studies that we report here recapitulates the California protocol's workflow for similar vacuum filtration and optical microscopy measurements. We intend our observations to inform practitioners in the field who are carrying out collect-and-transfer workflows with optical microscopy end-points. Although not the focus of this study, our results may inform preparation of samples on analytical filters for spectroscopic analyses, but comparisons of spectroscopy performance are beyond this study's scope.

Our study started by comparing the ultrastructure of these filters to inform our observations of their filtration performance. SEM image analysis of the membranes' ultrastructure was consistent with our rank ordering of water permeance measurements. The thinnest membranes, MSSN-Au, showed the fastest absolute and surface area-normalized water flux rates, while the thickest membranes, PSi, showed the slowest absolute and surface area-normalized flux rates. SEM imaging additionally revealed the variety of pore geometries of each membrane type. Despite being ~3.2- and ~3.9-times thicker than the other two polymeric membranes, PTFE had the fastest absolute and surface area-normalized flow rates of the three compared polymeric filters. The PTFE ultrastructure we observed (see row 4 of Figure 1) revealed that PTFE membranes likely have the highest porosity of all five compared membrane types. Given the challenges already noted and likely for similar reasons, we and their vendor are unable to provide a porosity value for PTFE. Nevertheless, the micrographs in Figure 1 support an effective highest porosity for PTFE. Even with its higher effective porosity over MSSN-Au, the latter demonstrated ~24-times higher surface area-normalized flow rates vs. PTFE since MSSN-Au is 89-times thinner than PTFE. These results are expected given water permeance is inversely dependent on membrane thickness,

in addition to other membrane properties (e.g., porosity, internal surface area) (14). When choosing a filtration membrane for MP capture and analysis, practitioners thus may be better served by opting for thinner membranes and/or membranes with more discrete pore geometry. While polymeric membranes such as PTFE and PCTE generally offer adequate water permeance for clean samples (e.g., drinking water) at reasonable cost, these two filter types come with less ideal optical imaging properties (see below).

One limitation of our study is that we challenged the filters with clean and relatively low particle burden samples. Field samples, whether they be drinking water or environmental water samples, will undoubtedly have higher particle burdens and thus effective filtration rates will be lower than those reported here. Nevertheless, our results help inform filter choice when processing various types of samples with suspected MP contamination. We note that all the filters compared during this study have been used to analyze field samples and that the controlled conditions under which we tested filtration and imaging performance will help practitioners decide what filters may be suitable for certain applications. For instance, given its > two-hour processing time for one-liter of particle-free water, PSi filters are likely impractical for field samples with any appreciable particle loads, although others report using them for spectroscopic MP analysis with extensive sample preparation procedures (15, 16). PTFE and PCTE filters are commonly used in MP sample processing, as their abundance of surface area, porosity, and low cost, are generally supportive of this application (8, 10). However, the underlying heterogeneous pore geometry and material composition detract from the utility of these filters to support high-resolution optical microscopy, as our observations show they are prone to light scattering and auto-fluorescence.

The overall surface area and porosity of the membranes are also worth noting. Since MP and other particles will follow the path of least fluidic resistance, they tend to occupy pores when captured by the membrane (12, 17). The optical images shown in Figure 2 demonstrate this particle capture behavior. While MSSN-Au membranes demonstrated the highest surface area-normalized water flux rates, these membranes have only ~5% of the effective surface area (with fewer pores in absolute terms) than any of the polymeric filters examined. Although not investigated here, the collection of captured particles onto a small amount of membrane surface area could potentially decrease overall sample analysis time by reducing the time it takes the practitioner to find and to analyze captured particles across the filter. This “concentration factor” is worthy of future exploration, especially if combined with representative subsampling methods (18), to assess potential overall analytical time-savings. Still, practitioners must keep in mind overall filter loading and will want to consider total time needed to locate and to analyze particles, depending on their intended post-capture interrogation methods. Madejski and colleagues used a non-gold-coated variant of MSSN membranes to enumerate the entrainment of MPs throughout a municipal drinking water system (12), supporting the potential benefits of the concentration factor concept. While this theorized concentration factor benefit needs further empirical verification, using MSSN-Au membranes for subsampling analyses may come with a trade-off of lower overall absolute particle capture since MSSN-Au membranes have fewer pores (when compared to other filters) with which to capture particles. With respect to optical imaging properties, our observations found PTFE Background auto-fluorescence prevented use of higher gain to

improve contrast, limiting the image resolution of captured particles. Comparing PCTE and PCTEG, the gold coating of this polymeric membrane apparently improves microscopy performance, most likely due to reducing light scatter and suppressing the membrane's inherent auto-fluorescence (as noted by others (19)). This benefit comes with a considerable reduction in sample processing, with ~4.0-fold lower flux rates and an ~8.9X increase in cost. These polymeric membranes, along with PTFE, also suffer from unavoidable wrinkling that happens when handling these filters during vacuum filtration setup and post-filtration retrieval of the filter. Such wrinkling was not observed for PS and MSSN-Au filters, given their different construction.

The inorganic composition of PS and MSSN-Au membranes likely prevents them from exhibiting appreciable auto-fluorescence. These inorganic filters are also more complicated to manufacture than polymeric filters (11, 20), so inorganic filters may remain more expensive than their polymeric counterparts. Considering the prices of the filters we examined, however, shows that PS, MSSN-Au, and PCTEG are nearly equivalently priced. Moreover, if the proposed concentration factor benefits described above hold for MSSN-Au, then their higher prices may be justifiable since their use may reduce overall analysis cost per sample. Finally, we note that the thinness, discrete pore geometry, and metal coating of MSSN-Au membranes likely endows them with optical characteristics supportive of ideal microscopy performance. Given the above considerations, practitioners will have to decide between sample processing versus optical microscopy performance when evaluating filters for their particular MP analytical work streams. For instance, our results suggest that practitioners may want to use metalized membranes due to their better visual microscopy performance over their non-metalized counterparts, and in cases where spectroscopic compositional analysis is required after visual microscopic counting and classification of captured particles, metalized membranes come with the added benefit of spectroscopy compatibility.

5. Conclusions

This study undertook a comparison of the filtration and optical imaging properties of five filter types for use in MP capture and analysis applications. We hope our study informs practitioners of the factors they should consider when evaluating their choice of filter. Given our results, we recommend that practitioners weigh the benefits and costs between sample processing and optical microscopy performance. Practitioners will also need to evaluate these factors in the light of standardized operating protocols, which may specify the type of filter(s) to be used for MP analysis, as mandated by regulatory authorities.

Acknowledgements

This work was supported by NIH Grant No. NIEHS 2-R44-ES031036-02 awarded to SiMPore Inc. The authors thank Drs. Steve Weisberg and Charles Wong of the Southern California Coastal Water Research Project for inclusion of this work in the SCCWRP interlaboratory methods comparison study. Electron microscopy imaging was performed in the Integrated Nanosystems Center (URnano) at the University of Rochester. Microfabrication was carried out at the Semiconductor and Microsystems Fabrication Laboratory (SMFL) at the Rochester Institute of Technology.

Bibliography

1. Koelmans AA, Mohamed Nor NH, Hermsen E, Kooi M, Mintenig SM, De France J. Microplastics in freshwaters and drinking water: Critical review and assessment of data quality. Water Res. 2019;155:410–22. Epub 2019/03/13. doi: 10.1016/j.watres.2019.02.054. [PubMed: 30861380]
2. Kwon JH, Kim JW, Pham TD, Tarafdar A, Hong S, Chun SH, Lee SH, Kang DY, Kim JY, Kim SB, Jung J. Microplastics in Food: A Review on Analytical Methods and Challenges. Int J Environ Res Public Health. 2020;17(18). Epub 2020/09/19. doi: 10.3390/ijerph17186710.
3. Ragusa A, Svelato A, Santacroce C, Catalano P, Notarstefano V, Carnevali O, Papa F, Rongioletti MCA, Baiocco F, Draghi S. Plasticenta: First evidence of microplastics in human placenta. Environment International.146:106274.
4. Schwabl P, Köppel S, Königshofer P, Bucsics T, Trauner M, Reiberger T, Liebmann B. Detection of various microplastics in human stool: a prospective case series. Annals of internal medicine. 2019;171(7):453–7. [PubMed: 31476765]
5. Leslie HA, van Velzen MJM, Brandsma SH, Vethaak AD, Garcia-Vallejo JJ, Lamoree MH. Discovery and quantification of plastic particle pollution in human blood. Environ Int. 2022;163:107199. Epub 2022/04/04. doi: 10.1016/j.envint.2022.107199. [PubMed: 35367073]
6. Hirt N, Body-Malapel M. Immunotoxicity and intestinal effects of nano- and microplastics: a review of the literature. Part Fibre Toxicol. 2020;17(1):57. Epub 2020/11/14. doi: 10.1186/s12989-020-00387-7. [PubMed: 33183327]
7. Yong CQY, Valiyaveettil S, Tang BL. Toxicity of Microplastics and Nanoplastics in Mammalian Systems. Int J Environ Res Public Health. 2020;17(5). Epub 2020/03/01. doi: 10.3390/ijerph17051509.
8. Schymanski D, Oßmann BE, Benismail N, Boukerma K, Dallmann G, von der Esch E, Fischer D, Fischer F, Gilliland D, Glas K, Hofmann T, Käppler A, Lacorte S, Marco J, Rakwe ME, Weisser J, Witzig C, Zumbülte N, Ivleva NP. Analysis of microplastics in drinking water and other clean water samples with micro-Raman and micro-infrared spectroscopy: minimum requirements and best practice guidelines. Anal Bioanal Chem. 2021;413(24):5969–94. Epub 2021/07/21. doi: 10.1007/s00216-021-03498-y. [PubMed: 34283280]
9. De Frond H, Thornton Hampton L, Kotar S, Gesulga K, Matuch C, Lao W, Weisberg SB, Wong CS, Rochman CM. Monitoring microplastics in drinking water: An interlaboratory study to inform effective methods for quantifying and characterizing microplastics. Chemosphere. 2022;298:134282. doi: 10.1016/j.chemosphere.2022.134282. [PubMed: 35283150]
10. Primpke S, Christiansen SH, Cowger W, De Frond H, Deshpande A, Fischer M, Holland EB, Meyns M, O'Donnell BA, Ossmann BE, Pittroff M, Sarau G, Scholz-Böttcher BM, Wiggin KJ. Critical Assessment of Analytical Methods for the Harmonized and Cost-Efficient Analysis of Microplastics. Appl Spectrosc. 2020;74(9):1012–47. Epub 2020/04/07. doi: 10.1177/0003702820921465. [PubMed: 32249594]
11. Wright E, Miller JJ, Csordas M, Gosselin AR, Carter JA, McGrath JL, Latulippe DR, Roussie JA. Development of isoporous microslit silicon nitride membranes for sterile filtration applications. Biotechnology and Bioengineering. 2019.
12. Madejski GR, Ahmad SD, Musgrave J, Flax J, Madejski JG, Rowley DA, DeLouise LA, Berger AJ, Knox WH, McGrath JL. Silicon Nanomembrane Filtration and Imaging for the Evaluation of Microplastic Entrainment along a Municipal Water Delivery Route. Sustainability. 2020;12(24):10655. [PubMed: 36938128]
13. Almuhtaram H, Andrews RC. Sampling Microplastics in Water Matrices: A Need for Standardization. ACS ES&T Water. 2022;2(8):1276–8. doi: 10.1021/acsestwater.2c00236.
14. Gaborski TR, Snyder JL, Striemer CC, Fang DZ, Hoffman M, Fauchet PM, McGrath JL. High-performance separation of nanoparticles with ultrathin porous nanocrystalline silicon membranes. ACS Nano. 2010;4(11):6973–81. Epub 2010/11/04. doi: 10.1021/nn102064c. [PubMed: 21043434]
15. Da Costa Filho PA, Andrey D, Eriksen B, Peixoto RP, Carreres BM, Ambühl ME, Descarrega JB, Dubascoux S, Zbinden P, Panchaud A, Poitevin E. Detection and characterization of small-sized microplastics (≥ 5 μm) in milk products. Scientific Reports. 2021;11(1):24046. doi: 10.1038/s41598-02103458-7. [PubMed: 34911996]

16. Weber F, Kerpen J, Wolff S, Langer R, Eschweiler V. Investigation of microplastics contamination in drinking water of a German city. Science of The Total Environment. 2021;755:143421. doi: 10.1016/j.scitotenv.2020.143421. [PubMed: 33183796]

17. Smith KJ, May M, Baltus R, McGrath JL. A predictive model of separations in dead-end filtration with ultrathin membranes. Separation and Purification Technology. 2017;189:40–7.

18. De Frond H, O'Brien AM, Rochman CM. Representative subsampling methods for the chemical identification of microplastic particles in environmental samples. Chemosphere. 2023;310:136772. doi: 10.1016/j.chemosphere.2022.136772. [PubMed: 36220434]

19. Oßmann BE, Sarau G, Schmitt SW, Holtmannspötter H, Christiansen SH, Dicke W. Development of an optimal filter substrate for the identification of small microplastic particles in food by micro-Raman spectroscopy. Anal Bioanal Chem. 2017;409(16):4099–109. Epub 2017/04/26. doi: 10.1007/s00216-017-0358-y. [PubMed: 28439620]

20. Langner A, Müller F, Gösele U. Macroporous Silicon. Molecular- and Nano-Tubes2011. p. 431–60.

Highlights

- One of the most widely used methods for the analysis of microplastics involves capture and on-filter interrogation by optical microscopy.
- Practices in this field are moving toward greater standardization and harmonization, requiring better understanding of the performance characteristics of analytical methods.
- The filtration and optical microscopy performance of five analytical filters is reported, along with related factors that practitioners should consider when evaluating filters for microplastics analysis.

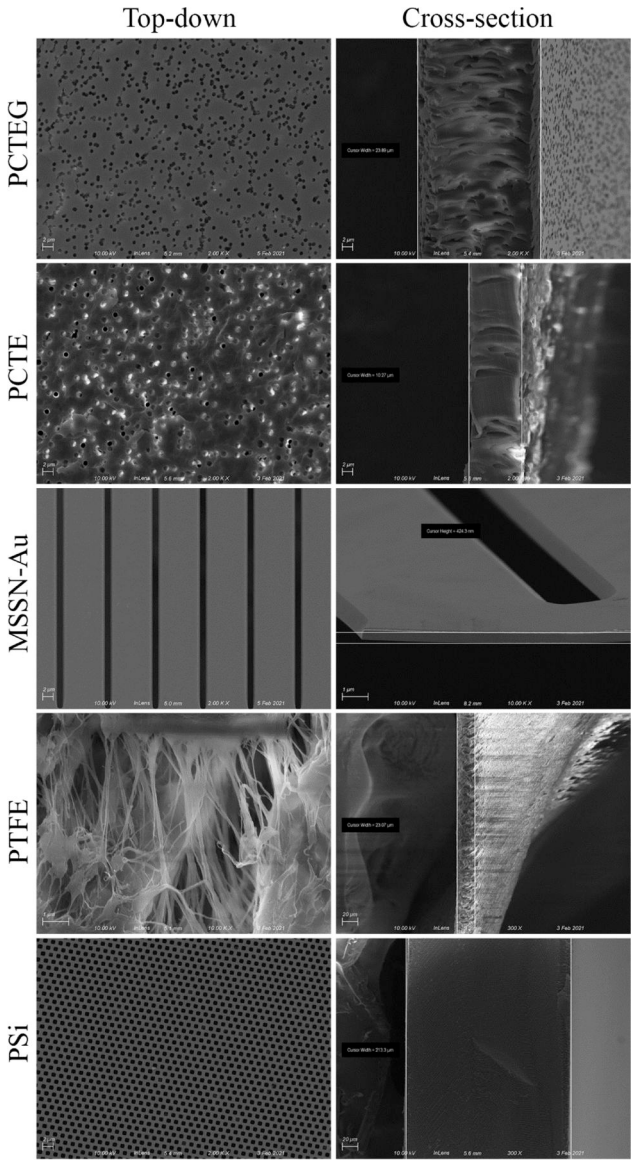

Figure 1:

Scanning electron microscopy imaging of five filter types. Representative micrographs are shown for top-down (left) and cross-sectional (right) views. Image magnification ranged from 300X to 10,000X at 10–20kV acceleration voltage (depending on membrane type).

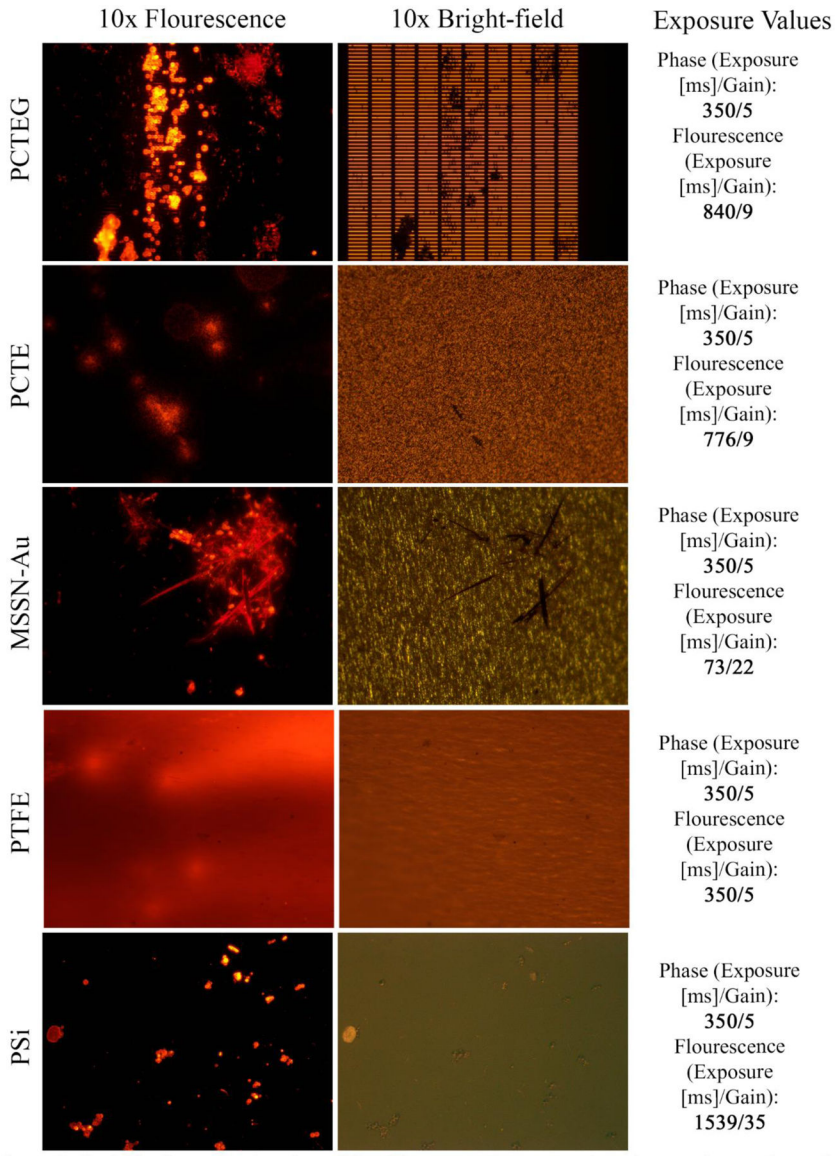

Figure 2:

Optical microscopy imaging of five filter types. Representative micrographs are shown for fluorescence (left), fluorescence-illuminated bright-field (middle), and related image acquisition data (right). Exposure time and camera gain settings are reported for each fluorescent image.

Table 1:

General Information and Key Properties of Filters

Filter Type	Vendor	Cat. No.	Lot No.	Composition	Cut-off	Porosity	Thickness	Retail Price/ Filter (USD)
PTFE	ADVANTEC	H100A025A	90227640	Polytetrafluoro ethylene hydrophobic-treated	1.0 μm	UNK	35 μm	$3.33
PCTE	Sterlitech	PCT1025100	M-180227	Polycarbonate	1.0 μm	16%	11 μm	$0.96
PCTEG	Sterlitech	1270007	TPA.PC.2001.I.8	Polycarbonate 40 nm gold-coated	0.8 μm	15%	9 μm	$24.79
PSi	Smart Membranes	950789-W16	UNK	Silicon	1.0 μm	~60%	220 μm	$30.00
MSSN-Au	SiMPore	MSSN400-3L-1.0-Au	4882	Silicon nitride 120 nm gold-coated	1.1 μm	13%	0.5 μm	$30.00

Notes:

1. Abbreviations: polytetrafluoroethylene (PTFE), polycarbonate track-etched (PCTE), polycarbonate track-etched gold-coated (PCTEG), porous silicon (PSi), microslit silicon nitride gold-coated (MSSN-Au)

2. As of 10/19/2022, ADVANTEC Cat. No. H100A025A has been discontinued and replaced by Cat. No. T100A025A.

3. Cut-off (i.e., pore size), thickness and porosity determined from SEM measurements for MSSN-Au; all other values as reported by vendors.

4. Listed prices were calculated per-filter based on variable minimum order quantity as of 10/19/2022.

Table 2:

Water Permeance Results by Filter Type

Filter	1 L Water Flux Time @ 97.9 kPa (min)	Absolute Water Flow Rate (mL • min^{-1})	Area-normalize Water Flow Rate (mL • min^{-1} • mm^{-2})	Effective Filter Surface Area (mm^2)
PTFE	7.79 ± 0.07	128 ± 1.14	1.05	122.7
PCTE	9.37 ± 0.21	107 ± 2.37	0.87	122.7
PCTEG	37.8 ± 1.17	26.4 ± 0.82	0.22	122.7
PS	148 ± 3.53	6.76 ± 0.16	0.07	100.0
MSSN-Au	6.39 ± 0.17	156 ± 4.11	24.8	6.3

Notes:

1. Abbreviations: polytetrafluoroethylene (PTFE), polycarbonate track-etched (PCTE), polycarbonate track-etched gold-coated (PCTEG), porous silicon (PSi), microslit silicon nitride gold-coated (MSSN-Au).

2. One-liter timed passage data are reported as mean ± standard deviation (n = 3). Absolute flow rate data are reported as *mean passage time / 1,000 ± coefficient of variation*, and those values were further divided by membrane surface area to calculate surface area-normalized flow rates.